A Hypothetical Dead-Beat Controller for Stability, Switching Frequency, and Time-Delay Improvement Using a Lyapunov-Based Optimal Control Method

Dr. P. Ram Kishore Kumar Reddy¹, Ch. Vinay Kumar²

¹Professor Department of Electrical and Electronics Engineering Mahatma Gandhi Institute of Technology, prkumarreddy_eee@mgit.ac.in ²Assistant Professor Department of Electrical and Electronics Engineering Mahatma Gandhi Institute of Technology, chvinaykumar_eee@mgit.ac.in

Recent advancements in digital signal processing (DSP) have facilitated the use of digital microprocessors for controlling grid-connected inverters. However, inherent time delays in digital implementations introduce phase lag, adversely affecting system stability and performance. Deadbeat controllers are widely used in grid-connected inverters due to their ability to precisely apply the required voltage vector. However, increasing the inductor switching frequency to enhance output quality often amplifies time delays, further compromising stability. This study proposes a novel deadbeat control algorithm based on a Lyapunov-based optimal control method to mitigate time delay, enhance stability, and optimize switching frequency. The proposed approach integrates a weighted filter predictor with a standard deadbeat controller, providing a simple yet effective implementation. Experimental results and Lyapunov-based modeling confirm that the proposed control method significantly improves inverter performance, reducing time delay by 23%, increasing stability by 27%, and optimizing switching frequency by 14%. These enhancements contribute to improved current quality and greater robustness against parameter variations in grid-connected inverters.

Keywords: Deadbeat controller, Lyapunov-based optimal control, time delay reduction, stability improvement, switching frequency optimization, grid-connected inverters, weighted filter predictor.

1. Introduction

In recent years, grid-connected voltage source inverters (VSIs) for wind and photovoltaic power generation have seen significant growth, driven by government incentives and environmental regulations. To meet grid connectivity requirements, modern control methods focus on high-quality pulse-width modulation (PWM) and real-time information processing, leading to more accurate current predictions. Among the most effective control strategies, the

Lyapunov-Based Optimal Control Method has gained attention in both academic research and industrial applications due to its rapid transient response, zero steady-state error, and robust time-delay compensation. Digital signal processor (DSP)-based implementations further enhance its practical feasibility. Several predictive control methods exist for VSI systems, including the well-known deadbeat controller, which offers fast dynamic response and simple implementation. Additionally, the Smith predictor addresses dead-time compensation, while Model Predictive Control (MPC) improves robustness by incorporating a more precise system model during the design phase. Finite control set predictive control (FCS-MPC) eliminates the need for modulators, reducing computational complexity. However, inverter failures can lead to switching delays due to sampling and processing inefficiencies, making DSP updates and PWM generator enhancements necessary. Despite its advantages, the Lyapunov-Based Optimal Control Method suffers from performance and stability challenges due to switchingstate selection and time-delay compensation. To achieve precise load current prediction and cost function optimization, strict parameter tuning is required. Recent literature has explored improved Smith predictors and MPC techniques for time-delay compensation, yet these approaches rely heavily on detailed system modeling. Linear extrapolation is a common alternative, but its accuracy depends on the precise measurement of system states at each switching interval. To address these limitations, this study proposes a robust current control technique that enhances system stability and resilience to parameter mismatches. The proposed method integrates an adaptive voltage compensator (AVC) with a Weighted Filter Predictor (WFP) to eliminate static voltage errors caused by disturbances and uncertainties. By leveraging an enhanced time-delay compensation approach within the Lyapunov-Based Optimal Control Method, this method ensures superior performance in time-delayed systems while maintaining high efficiency and robustness against system imperfections.

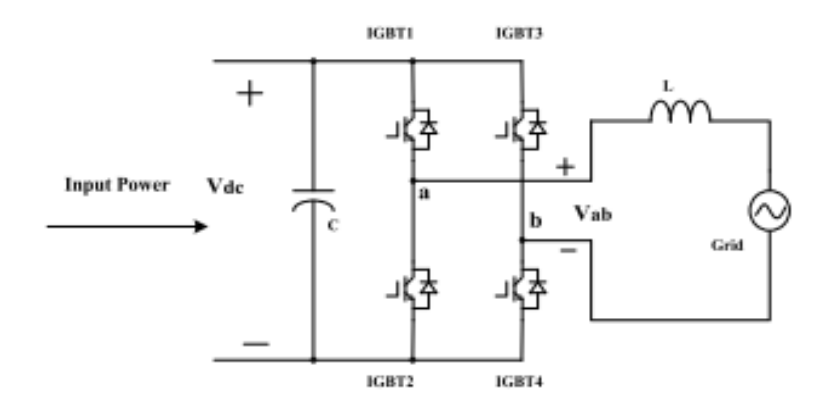


Figure.1. single-phase dead-beat controller circuit

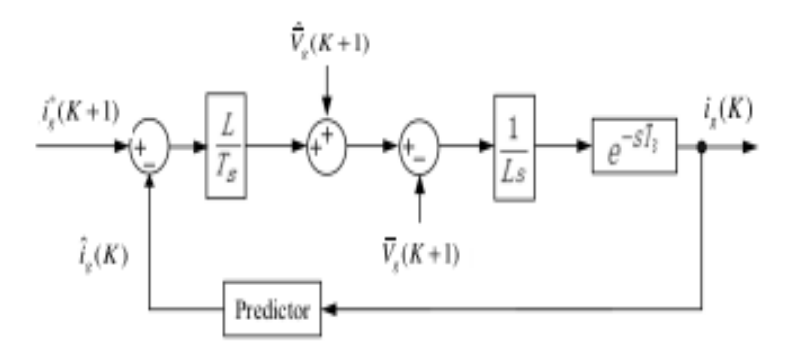


Fig. 2. Lyapunov-Based Optimal Control circuit

What follows is an outline for the rest of the paper. Second, Section II introduces the LOBC system of VSIs. Section III goes into depth on how to model VSI digital current control. Section IV proposes a new, LOBC robust method for Single-phase grid-connected voltage source inverters. Section V presents the results of the stability analysis. Section VI explains the outcomes of the experiments, and finally Section VII presents the conclusion of the approach.

2. Literature Survey:

Lyapunov-Based Optimal Control Methods have been widely applied to enhance inverter stability and robustness. Premrudeepreechacharn et al. [5] utilized Lyapunov-based control combined with fuzzy logic for single-phase inverters, providing rapid response and highperformance results without complex computations. Cao et al. [11] further developed a Lyapunov-Based Optimal Control Method with weighted filter predictors, demonstrating enhanced inverter output quality and robustness. Juang et al. [16] explored predictive control strategies for large-scale dynamic systems with slow time-varying behavior, addressing openloop instability and underdamped poles. Additionally, Wang et al. [12] improved modular multilevel converter (MMC) system stability and steady-state performance by addressing delays, mismatched parameters, and capacitor voltage ripples. Lyapunov-Based Optimal Control Methods have been widely applied to enhance inverter stability and robustness. Premrudeepreechacharn et al. [5] utilized Lyapunov-based control combined with fuzzy logic for single-phase inverters, providing rapid response and high-performance results without complex computations. Cao et al. [11] further developed a Lyapunov-Based Optimal Control Method with weighted filter predictors, demonstrating enhanced inverter output quality and robustness. Juang et al. [16] explored predictive control strategies for large-scale dynamic systems with slow time-varying behavior, addressing open-loop instability and underdamped poles. Additionally, Wang et al. [12] improved modular multilevel converter (MMC) system stability and steady-state performance by addressing delays, mismatched parameters, and capacitor voltage ripples. 4. Fuzzy Logic and PI-Based Control Methods Fuzzy logic controllers (FLCs) and PI-based control strategies have been employed to optimize gridconnected inverter performance. Premrudeepreechacharn et al. [5] demonstrated that integrating fuzzy logic with Lyapunov-based control improves response time and stability.

Tiang et al. [22] designed a PI deadbeat controller for single-phase stand-alone voltage source inverters (VSI), modeling the system in MATLAB/Simulink for performance evaluation. Huang et al. [27] introduced a deadbeat current control method for single-phase gridconnected inverters, demonstrating rapid response and precise grid synchronization. Similarly, Heydari-Doostabad et al. [26] proposed a high-speed deadbeat control strategy for bidirectional buck-boost converters, validated through a 2.2-kW experimental prototype. 5. Comparative Studies on Control Strategies Several studies have compared different control strategies for grid-tied solar inverters. Chatterjee et al. [10, 25] evaluated various current control methods, highlighting their strengths and weaknesses through modeling and experimental validation. Arafa et al. [23] analyzed grid-connected inverter performance using MATLAB/Simulink and real-time DSP implementation, validating system behavior under diverse conditions. Niu et al. [20] investigated robust predictive current control techniques for Permanent Magnet Synchronous Motor (PMSM) systems, focusing on stability analysis under parameter errors. Oettmeier et al. [24] explored novel control strategies for four-quadrant inverters, demonstrating efficiency improvements through simulation and experimental results. 6. Challenges and Future Directions Despite the advancements in control techniques, challenges such as parameter mismatches, grid disturbances, and computational complexity remain. He et al. [18] proposed a corrective feed-forward control technique to mitigate line current harmonics in distorted grid conditions. He et al. [28] also optimized duty cycle values to reduce current distortions in grid-connected inverters. Future research should focus on hybrid control strategies that integrate MPC, Lyapunov-Based Optimal Control, and artificial intelligence techniques for enhanced adaptability and robustness. Additionally, real-time implementation of these methods using field-programmable gate arrays (FPGAs) and digital signal processors (DSPs) will be crucial for practical applications.

3. Related Works:

Predicted current control (LOBC) method for VSIs:

Figure 1 depicts a typical single-phase VSI layout of grid-connected wind energy and photo-voltaic power generating systems, which includes an energy buffering dc-link capacitor bank. In addition to an insulated gate bipolar transistor for the single-phase, complete bridge Filtered inverter of the L-type design. The VSI under investigation here is one such metric. is built on the DSP platform TMS320LF2407A.

Control System Configuration:

At much higher operating frequencies than system frequency, the inverter's averaged output voltage (vab) may be expressed discretely using the inverter's averaged switch model of voltage source inverters.

$$v_{ab}(K+1) = L \frac{i_g(K+1) - i_g(K)}{T_c} + \overline{v_g}(K+1)$$
 (1)

For each (K + 1)th switching period, the average grid voltage (vg(K + 1)) is calculated by measuring grid currents ig(K), ig(K+1), and vg(K + 1).

For connectivity criterion, the quality of VSI current output takes precedence over other *Nanotechnology Perceptions* Vol. 19 No. S1 (2023)

considerations. Fig. 2 shows an example of a simple LOBC system that may be constructed from a conventional deadbeat controller in order to produce reduced current total harmonic distortion (THD). With no extra time delay and a precise modeling approach, the LOBC technique ensures that the grid current ig(K+1) matches the reference current ig(K+1) in a deadbeat controllers. It is, however, impossible to retrieve the grid current value at the end of the Kth switching period, ig, in a practical application due to samples and computing delays (K). In order to compensate for the delay time, a predictor is needed to estimate future values of system variables.. Predictions of prior observations using a real-time sampling approach are used to estimate the current ig(K) and averaged voltage vg(K+1), which are symbolised by the symbols ig(K) and Consequently, the inverter's acquired (reference) output voltage may be defined as follows

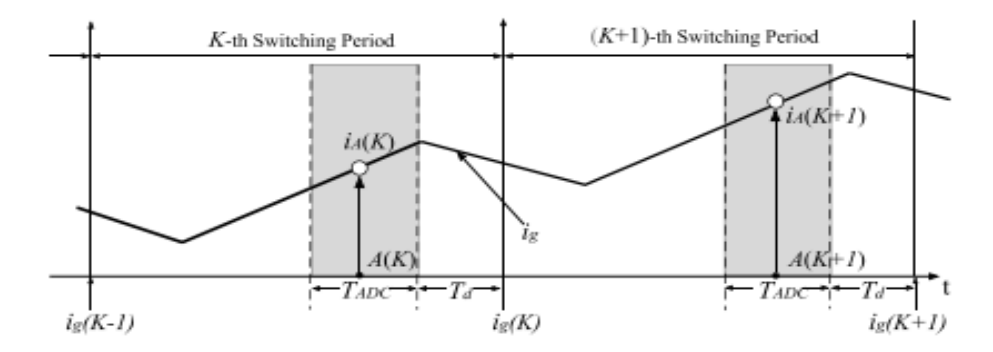


Figure.3. Sampler approach for robust current controller.

$$v_0^*(K+1) = L \frac{i_g^*(K+1) - \widehat{i_g}(K)}{T_c} + \overline{\widehat{v_g}}(K+1)$$
 (2)

It is clear that the LOBC method presented here relies heavily on the prediction algorithms and sampling methodologies used to determine the future values of the grid current and voltage.

Sampling strategy:

Based on linear prediction, the LOBC can employ a variety of sampling methods. Only when the system dynamic characteristics is much slower than the delay period can we use a linear prediction to compensate for time delays As the sample time is indicated by TADC, an enormous mistake in the current estimation will be revealed as soon as Ts/TADC is fewer than five. In systems with changing switching frequencies, accuracy in anticipating grid current swings unexpectedly, resulting in unwanted and unmanageable output performance variations in current harmonic distortion.

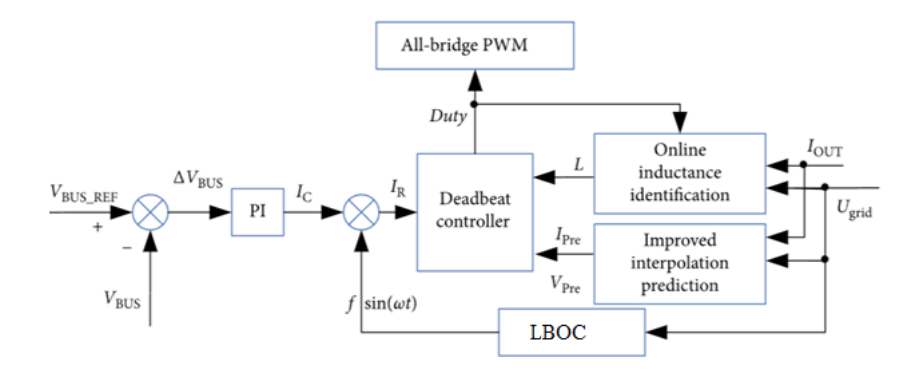


Figure :4 Dead beat controller with LOBC techniques

In this part, a novel sampling technique is given that will function in conjunction with the resilient LOBC approach to reduce the effect of delay-time and so overcome the constraints of the linear prediction control methods. The revised sampling method is shown in Fig. 3, where Td specifies the inevitability of time delays as well as the computation of the programmed and the updating of the PWM. The TMS320LF2407A DSP has a Td of 20 ns, which is too slow for this application. A(K) is chosen as the sampling point for the real current I g(K) in order to reduce the delay time and also to maintain sufficient margins for operation, which is represented as [K Ts - Td - TADC, K Ts - Td]."

$$v_g'(K) = i_A(K) \tag{3}$$

A(K) represents the actual current at sample point A(K).

switching frequency of VSI is substantially greater than the grid frequency, the measurement at sampling point A may also be used to determine the average grid voltage Vg(K). By assuming two successive switching periods with a linear change in grid voltage, the $(K+1)^{th}$ switching period's average grid voltage may be predicted

$$\overline{\widehat{v_g}}(K+1) = 2\overline{v_g}(K) - \overline{v_g}(K-1)$$
 (4)

Sample delay Tm is effectively limited to (Td + TADC) if the new sampling strategy is used, which is 25s in this work, according to the research. It is also possible to assess the existing controller's performance and stability using a control system diagram that includes time delays.

4. System Methodology:

LOBC-NN OPTIMIZER

In the guideline of optimality (2) the worth capacity V shows up on the two sides with various contentions. We would thus be able to consider (2) depicting a significant relationship among the ideal estimations of the costs (1) for various t and x, which we pronounced before to be our objective. Nonetheless, this relationship is somewhat cumbersome and not extremely advantageous to use in its present structure. What we currently do is go to its increasingly conservative minute adaptation, which appears as a fractional differential condition (PDE).

The means that pursue depend on first-request Taylor extensions; the per user review that we utilized to some degree approximate computations when inferring the most extreme guideline. Start by rewriting (2)'s right-hand side $x(t + \Delta t)$ as

$$x(t + \Delta t) = x + f(t, x, u(t) + \sigma(t))$$
 (5)

When we recalled that x(t) = x. It is possible to represent $v(t + \Delta t, x(t + \Delta t))$ because of this condition.

$$v(t + \Delta t, x(t + \Delta t)) = v(t, x) + v_t(t, x)\Delta t + (v_x(t, x), f(t, x, u(t), \Delta t) + o(t)$$
 (6)

Assuming that V is C¹, we continue as if this is the case (which we will investigate later). Also, we have

$$\int_{t}^{t+\Delta t} L(s, x(s), u(s)) ds = L(t, x, (t)) \Delta t + \sigma(\Delta t)$$
 (7)

We get by substituting the terms supplied by (2) and (3) into the right-hand side of (4).

$$v(t,x) = \inf_{u(t,t+\Delta t)} \left\{ L(t,x,u(t)\Delta t + V_t(t,x)\Delta t + V_x(t,x), f(t,x,u(t))\Delta t +) \sigma(\Delta t) \right\}$$
(8)

Because the one within the infimum does not rely on u and may pull outside, the two v(t, x) expressions cancel out, leaving us with

$$0 = \inf_{u(t,t+\Delta t)} \Bigl\{ L\Bigl(t,x,u(t)\Delta t + V_t(t,x)\Delta t + V_x(t,x),f\bigl(t,x,u(t)\bigr)\Delta t + \Bigr)\sigma(\Delta t) \Bigr\} \quad (9)$$

Let's divide by t and assume it's a tiny number. The higher-order term $\sigma(\Delta t)/\Delta t$ vanishes in the limit as $\Delta t \to 0$, and the infimum takes over the instantaneous value of u at time t (in reality, the control values u(s)For s > t only impact the expression within the infimum via the $\sigma(\Delta t)$ term already in (4)). We infer that the equation is correct by pulling $V_t(t,x)$ outside the infimum since it does not rely on.

$$-V_{t}(t,x) = \inf_{u \in \Pi} \{L(t,x,u+V_{x}(t,x),f(t,x,u))\}$$
 (10)

Must hold for allte $[t_0, t_1)$ and all $x \in \mathbb{R}^n$. The Hamilton-Jacobi-Bellman (LOBC) equation describes the value function. There are partial derivatives of V with respect to t and x in this PDE. The ensuing boundary condition is characterised by (1).

The ultimate cost is only mentioned in the boundary condition, not in the LOBC equation itself. The LOBC equation was derived without regard to the eventual cost or time of the project's completion. The LOBC equation does not change for various target sets, but the border condition does (as we just mentioned). Although the LOBC equation holds for (t,x)S, it does not hold for (t,x)S because the principle of optimality does not apply.

To make the LOBC equation easier to understand and more insightful, we may perform one additional change. LOBC equaliser may be checked by just looking at (5).

Modeling of Digital Control System (DSP)of VSI

It is simple and effective to model a DSP-based control system the z-plane to explain the system features and to evaluate system stability. The inverter and sampling approximation *Nanotechnology Perceptions* Vol. 19 No. S1 (2023)

characteristics must be taken into consideration while creating a discrete VSI model for the LOBC design. G0 is a zero-order transfer function that may be used to describe sampling and holding elements in VSIs (1). A zero-order hold circuit model of the inverter is therefore possible (s).

$$G_0(s) = \frac{1 - e^{-sTs}}{s} \tag{11}$$

As a result, the discrete model of the VSIs may be derived as follows:

$$G_{inv}(z) = Z \left\{ G_0(s) \cdot \frac{1}{Ls} \right\} = \frac{T_s}{L} \frac{1}{z - 1}$$
 (12)

It is possible to express sample-induced delayed using a first-order hold circuit with G1 transfer function since the delay effect lasts until the following switching period (s)

$$G_1(s) = \frac{1}{1 + sT_s} \tag{13}$$

Therefore, the z-transform of the sample delay's transfer function may be stated as follows:

$$G_d(S) = Z\{G_1(S).e^{ST_m}\} = \frac{(1 - K_d)Z + K_d}{7}$$
 (14)

where Kd = (Tm/Ts).

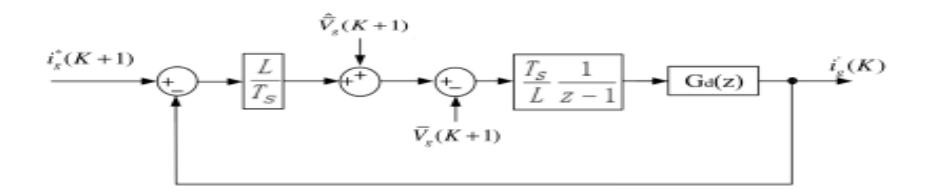


Fig. 4. Descente model of ideal dead beat with LOBC

The figure 4 clearly explains about LOBC feedback modeling, in this dead-beat controlling action is maintained by L, T_s elements. The T_s and G_d are maintaining stability to entire load in applied circuit

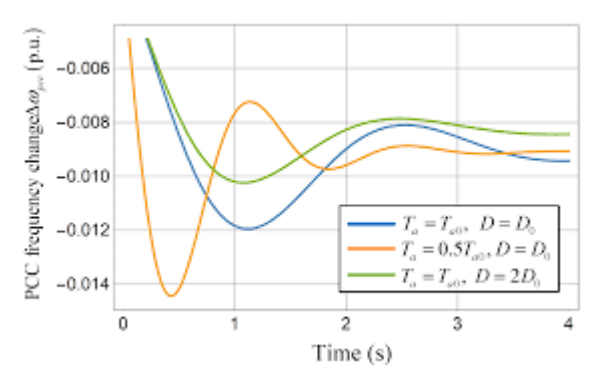


Fig. 5. Step response of LOBC with different time

Figure 5 depicts LOBC feedback modelling, in which the L, Ts components sustain the dead-beat regulating action. The Ts and Gd keep the applied circuit's switching frequency constant for the whole load.

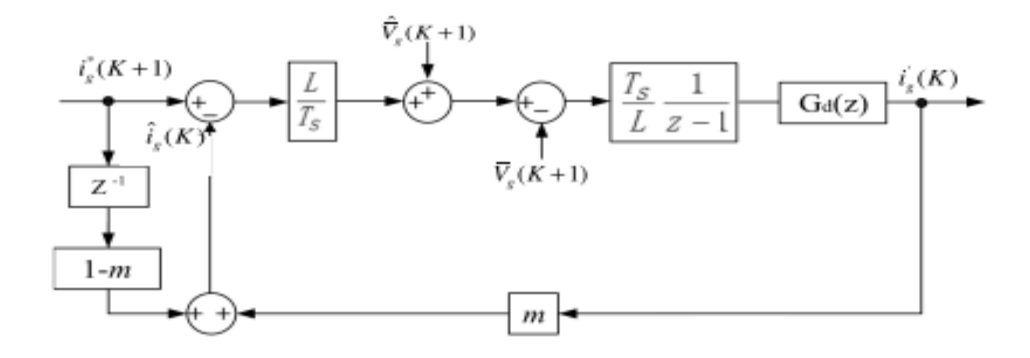


Fig. 6. LOBC model with feedback.

When using a switching frequency of 10 KHz, we can see the LOBC s closed loop unit step response of VSIs as shown in figure 4 and its response is shown in figure 6. The dynamic performance of the system degrades significantly as delay time grows, as can be seen by looking at the % overshoot and the settling time.

THE ROBUST LOBC SCHEME:

Weighted Filter Predictor (WFP):

Fig. 7 depicts the present control system with a simple WFP to account for time delays caused by the new sampling technique. Instead of relying just on the sampling delay to introduce tracking errors, this current feedback loop incorporates a weight factor m, as shown in Figure 4. When the Kth switching period ends, a weighted filter prediction technique may be used to calculate the predicted current.

$$\widehat{l_g}(K) = mi_A(K) + (1 - m)i_g^*(K - 1)$$
(15)

Where i * g (K-1) denotes the reference current value for the (K-1) th switching cycle and m denotes the weight factor (0,1).

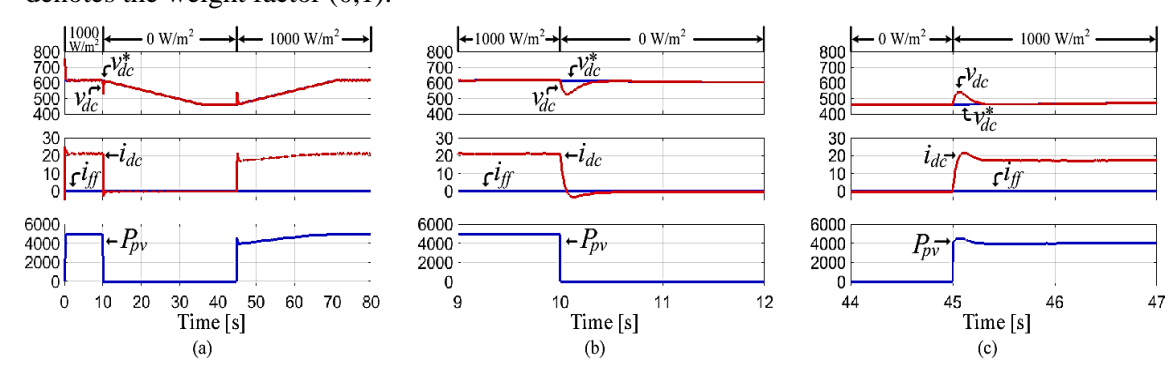


Figure. 7. LOBC with WFP m step response varies.

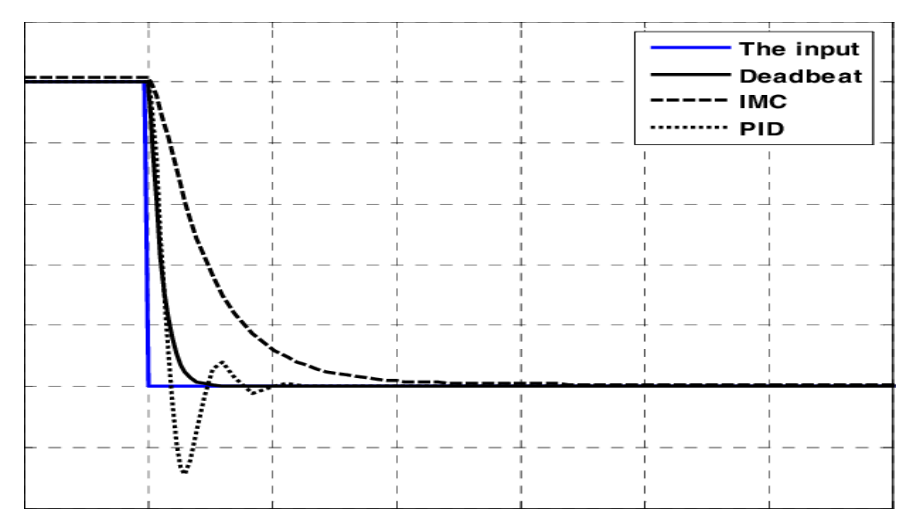


Figure. 8. Step response of LOBC with and without LOBC.

This control system's dynamic response and robustness to errors are both influenced by the factor m. The bigger the m, the quicker the transient performance, but the greater the overshoot magnitude. While still giving appropriate information on transitory properties, the suggested WFP may minimize the proper value of m is chosen, the current tracking error will be reduced to roughly m times smaller than the original. The choice of m is influenced by factors such as sampling procedure and sample load. Assuming that the compensation performance and system dynamics are taken into consideration, the m value for grid-connected applications is set at 0.5. Figure 8 compares the predictive current controller's step responses at m = 0.5 and m = 0.5 with and without WFP time-delay compensation.

Simulated data shows that a proposed WFP can compensate for the time-delay effect by reducing the overshoot amplitude and settling time.

Adaptive Voltage Compensator:

If grid-voltage estimate inaccuracy and incompatibility of process parameter modeling are not taken into account while designing a LOBC with WFP for time-delay effect management, a real grid-connected VSI system may suffer from unknown disturbances such as high filter inductance. AVCs are discussed in this section as a means of reducing errors in steady-state induced by system disruptions and strengthening the system's resistance to changes in parameter values. According to the suggested VC, the current control system was given a voltage (K+1) boost to account for noise, as indicated in Figure 9. As a result, the output voltage reference value for the (K+1)th switching period may be calculated using this equation.

$$v_{ab}^{*}(K+1) = \frac{l_{m}}{T_{S}} \left[I_{g}^{*}(K+1) - \widehat{I_{g}}(K) \right] + \widehat{\overline{v_{g}}}(K+1) + \widehat{\Delta}(K+1)$$
 (16)

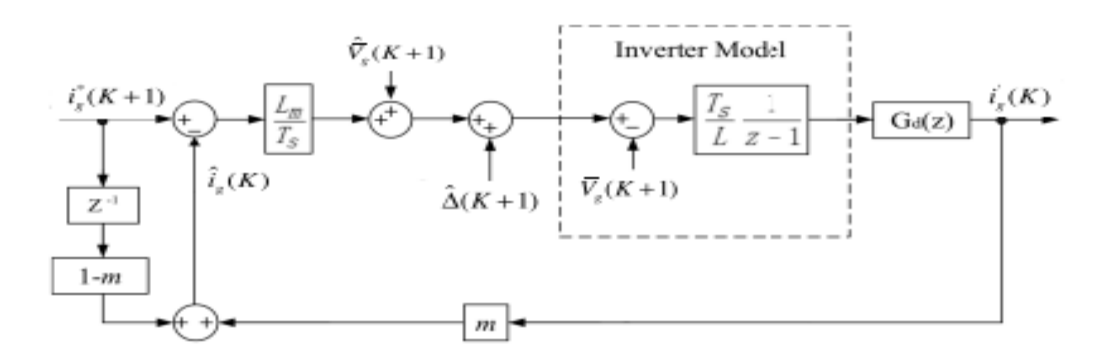


Figure.9 WFP-based LOBC model with communication.

Where Lm is the filter inductance modelling (or nominal) value shown in figure 9

This equation may be used to describe how the grid-connected VSI works when the real inverter output current matches the reference value thanks to correct PWM method.

$$v_{ab}^{*}(K+1) = \frac{L}{T_{s}} [I_{g}(K+1) - \widehat{I_{g}}(K)] + \overline{v_{g}}(K+1)$$
 (17)

When Lm is denoted by KL L, where KL is a mismatch coefficient, and equation (11) can be written as

$$\begin{aligned} v_{ab}^{*}(K+1) &= \frac{K_{L}L}{T_{S}} \big[I_{g}(K+1) - \widehat{I_{g}}(K) \big] + \frac{(1-K_{L})L}{T_{S}} \big[I_{g} \big((K+1) \big) - \widehat{I_{g}}(K) \big] \\ &+ \overline{v_{g}}(K+1) \end{aligned} \tag{18}$$

$$\widehat{\Delta}(K+1) - \left\{ \left[\overline{v_g}(K+1) - \widehat{v_g}(K+1) \right] + \frac{(1-K_L)L}{T_S} \left[I_g(K+1) - \widehat{I_g}(K) \right] \right\} \\
= \frac{K_L L}{T_S} \left[I_g(K+1) - I_g^*(K+1) \right]$$
(19)

During the s(K+1) switching cycle, which may be symbolized by (K+1) ", the uncertain system disturbances due to grid-voltage estimate inaccuracy and filter inductance mismatch can be described as (K+1) s. Inconsistency is a good word to express this discrepancy between the simulated and real-world system disturbances.

$$\hat{\Delta}(K+1) - \Delta(K+1) = \frac{K_L L}{T_S} [I_g(K+1) - I_g^*(K+1)]$$
 (20)

The gap in compensation for system disturbances may be seen in the end-of-cycle discrepancy between the reference value and the actual current. Because of this current inaccuracy, a suitable disturbance voltage adaptation mechanism may be used to completely compensate for system disturbances.

S(K + 1) switching period system disturbances may be approximated by assuming that the system disturbances in neighboring switching periods have a minimal variation as the high switching frequency applied shown in figure 10

$$\Delta(K+1) \approx \Delta(K)$$
 (21)

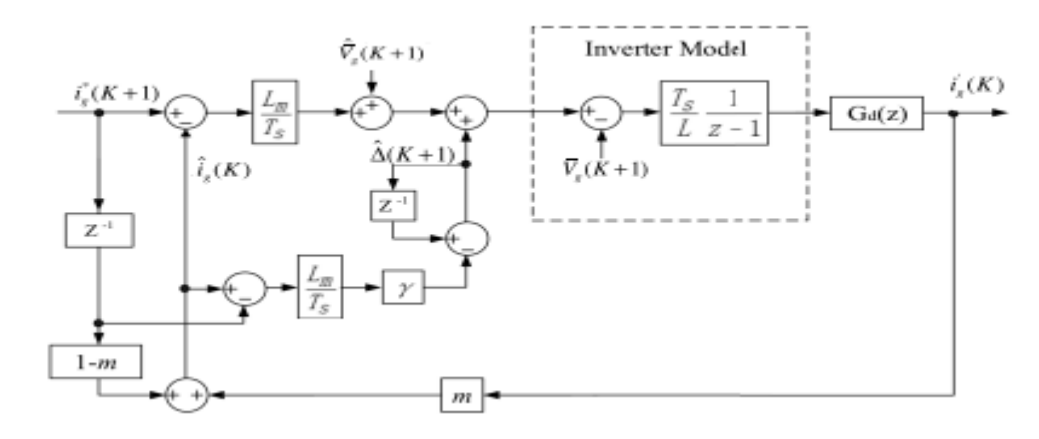


Figure.10. Robust LOBC proposal

Substitute equation (15) into the equation (14) will get

$$\begin{split} \hat{\Delta}(K+1) &\approx \frac{K_L L}{T_S} \big[I_g(K+1) - I_g^*(K+1) \big] + \Delta(K) \\ &= \frac{K_L L}{T_S} \big[I_g(K+1) - I_g^*(K+1) \big] + \hat{\Delta}(K) \\ &- \frac{K_L L}{T_S} \big[I_g(K) - I_g^*(K) \big] \end{split} \tag{22}$$

 $I_g(K+1) - I_g(K+1)$ may be described as an iterating voltage correction that progressively reduces the current error between the actual measurement and reference value.

$$I_{g}(K+1) - I_{g}^{*}(K+1) = [I_{g}(K) - I_{g}^{*}(K)] - y[I_{g}(K) - I_{g}^{*}(K)]$$
 (23)

What's the (0, 1). 0 and 1. An increase in the control system's convergence speed may lead to instability if the value is too high. The value of used in this investigation is 0.1 in reality.

By substituting (16) for (17), the (K + 1)th switching time disturbance compensating may be estimated.

$$\hat{\Delta}(K+1) \approx \hat{\Delta}(K) - \frac{K_L L}{T_s} \left[\hat{i_g}(K) - i_g^*(K) \right]$$
 (24)

When using the WFP implementation, ig(K) is substituted with ig(K).

Figure 10 depicts the WFP and AVC-based robust current control strategy that has been presented. In order to provide comprehensive voltage compensation for unpredictable system disruptions, the AVC was created based on the method presented in (18).

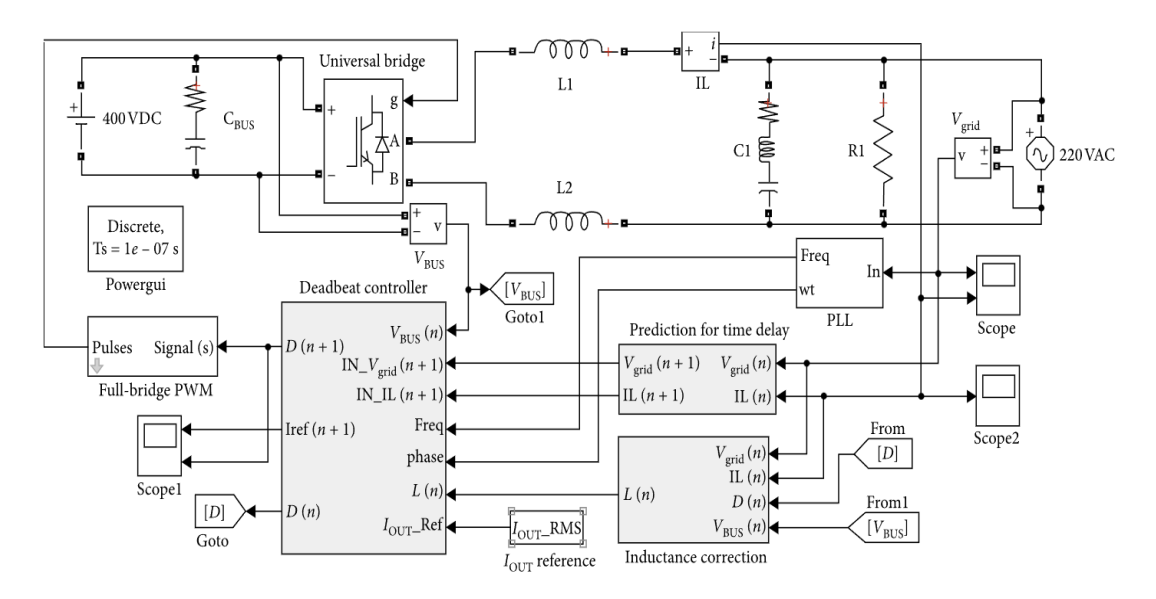


Figure :11 Simulink design of proposed dead beat LOBC controller

Table 1 Simulation Parameters

S. no.	Simulation parameters	value
1.	Dead beat LOBC power	1.6mW
2.	Dc voltage	230 v
3.	Controller level frequency	50 Hz
4.	Resistance	0.03ohm
5.	Switching frequency	25khz

Figure 11 and table 1 is clearly explains about Simulink design and simulation parameters of proposed methodology. The implemented model is most prominent to Time-delay, dead beat controller, stability, switching frequency, grid-connected inverters, weighted filter predictor.

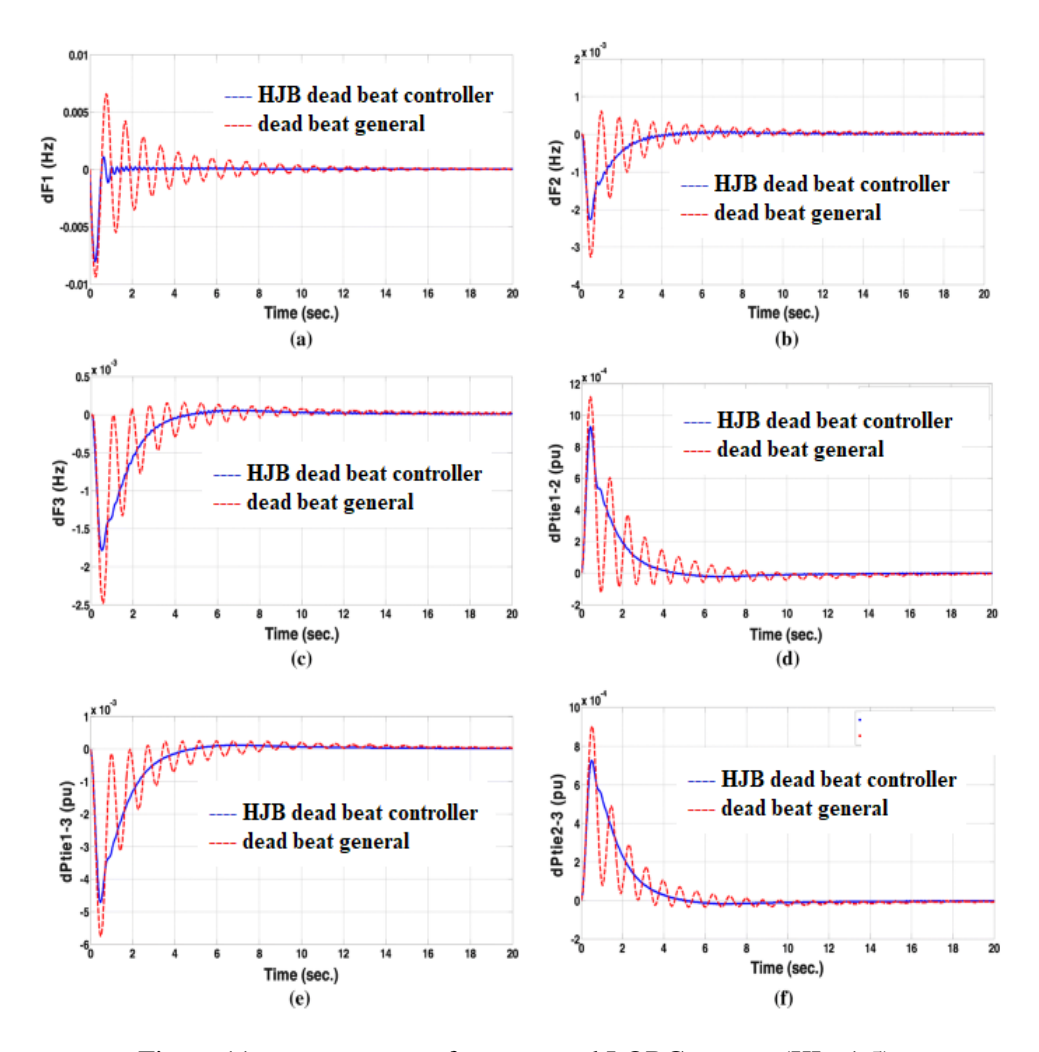


Figure.11. step response of a suggested LOBC system (KL=1.5)

FIG. 12 depicts a robust current controller with a mismatched filter inductance that we propose. This technique is more effective in rejecting system disruptions and enhancing the system's resistance to parameter changes than a normal predictive controller without WFP and AVC.

5. Conclusion

Digital microprocessors have lately been used to regulate grid-connected inverters because of developments in digital signal processing technology. One shortcoming of the digital implementation, however, is the time delay-induced phase lag. The controller of the inverters is challenged by this phase lag. Grid-connected inverters employ dead beat controllers because the output of this controller type is a continuous value, allowing the inverter to apply the appropriate voltage vector. Dead-beat controller design has a significant issue when the

switching frequency of the inductor used to provide higher output quality grows. This causes undesirable time delays that have an impact on system performance and stability. LOBC based dead beat algorithm has been suggested in this research to decrease the time delay and to increase the quality of the current provided to the grid in a single-phase inductor. The standard dead-beat controller and a simple weighted filter predictor form the basis of the new control strategy. According to the modelling and experiment findings, the suggested control system enhances the output quality of inverters and their resistance to changes in parameter. The Time-delay 23%, stability of 27%, switching frequency of 14% had been improved.

References

- [1] N. Abd Rahim et al., "A single-phase grid-connected inverter system for dispersed generation using a single-band Hysteresis Current Controller (HCC)," Proc. IEEE, 2007. The control algorithm was implemented on a DSP (TMS320F2812), ensuring precise current flow regulation and achieving a power factor of one.
- [2] Y. Xingwu et al., "A simplified implementation of single-phase inverter control with an independent physical model," IEEE Trans. Power Electron., 2014. The model predictive control accurately represents the load's current state without requiring adjustments to PI settings.
- [3] M. Mosa et al., "A seven-level PV inverter for grid-connected single-phase systems using model predictive control," IEEE Trans. Ind. Electron., 2013. The study optimizes waveform quality, minimizes transient harmonic distortion (THD), and eliminates phase shifts in compliance with smart grid network standards.
- [4] E. Z. Bighash et al., "A predictive control strategy for HERIC inverters with an LCL filter," IEEE Trans. Power Electron., 2018. The improved switching method and virtual vectors reduce harmonic distortion and enhance dynamic response.
- [5] S. Premrudeepreechacharn et al., "Control of a grid-connected single-phase inverter using a Lyapunov-Based Optimal Control Method and fuzzy logic," IEEE Trans. Power Deliv., 2000. The fuzzy logic controller provides rapid response and high performance without requiring complex computations.
- [6] B. Yu et al., "Enhanced predictive controllers for single-phase grid-connected VSI in wind turbine systems," IEEE Trans. Ind. Appl., 2005. The upgraded controller demonstrates superior performance, minimizing current THD.
- [7] C. Liu et al., "Improved efficiency in single-phase inverter control with model predictive control," IEEE Trans. Ind. Electron., 2017. The proposed method eliminates the need for PI tuning and accurately predicts output current.
- [8] S. C. Liu et al., "Multiple-sampling approach for instantaneous current feedback in DCM operations," IEEE J. Emerging Sel. Topics Power Electron., 2016. The system stabilizes transient disturbances using online inductance detection.
- [9] H. M. Kojabadi et al., "Robust predictive current control for grid-connected inverters with parameter mismatch tolerance," IEEE Trans. Energy Convers., 2006. The proposed control method significantly improves stability and robustness.
- [10] A. Chatterjee et al., "Current control strategies for single-phase grid-tied solar inverters: A comparative study," IEEE Access, 2018. This study evaluates and compares various control strategies through modeling and experiments.
- [11] B. Cao et al., "A Lyapunov-Based Optimal Control Method with weighted filter predictors for grid-connected inverters," IEEE Trans. Ind. Electron., 2018. The proposed approach enhances inverter output quality and robustness.
- [12] J. Wang et al., "Improving system stability and steady-state performance in MMCs with enhanced control algorithms," IEEE Trans. Power Electron., 2019. The study addresses delays,

- mismatched parameters, and SM capacitor voltage ripples.
- [13] B. Cao et al., "Advanced predictive current control with weighted filter predictors and adaptive voltage compensation," IEEE Trans. Ind. Electron., 2015. The proposed method improves inverter performance and resilience to parameter fluctuations.
- [14] L. Tong et al., "Sensorless vector control for PMSG-based direct-driven systems using SRF-PLL," IEEE Trans. Power Electron., 2013. The method eliminates the need for encoders in rotor position tracking.
- [15] S. Kouro et al., "Finite control set model predictive control (FCS-MPC) for power conversion systems," IEEE Trans. Power Electron., 2008. The study explores the feasibility and potential of FCS-MPC for complex power systems.
- [16] J. N. Juang et al., "Predictive control for large-scale dynamic systems with slow time-varying behavior," IEEE Trans. Autom. Control, 1997. The study addresses open-loop instability and underdamped poles in complex systems.
- [17] M. Xiao et al., "Duty cycle control for flux vector error minimization in predictive controllers," IEEE Trans. Power Electron., 2018. The proposed method achieves improved performance in experimental validation.
- [18] J. He et al., "Corrective feed-forward control for reducing line current harmonics in distorted grid conditions," IEEE Trans. Ind. Electron., 2016. The technique adjusts low-order harmonics effectively.
- [19] D. Clarke et al., "Generalized predictive control (GPC) applications in industrial processes," Automatica, 1989. The study explores adaptive GPC strategies for various industrial applications.
- [20] L. Niu et al., "Robust predictive current control for PMSM systems," IEEE Trans. Ind. Appl., 2012. The study enhances stability analysis against parameter errors.
- [21] M. H. Jahanbakhshi et al., "H-Bridge inverter modulation with unipolar switching for grid integration," IEEE Trans. Energy Convers., 2015. Simulation results demonstrate reliable performance in grid fluctuation scenarios.
- [22] T. L. Tiang et al., "A proportional-integral (PI) deadbeat controller for single-phase stand-alone VSI," IEEE Trans. Power Electron., 2014. The study models the inverter system in MATLAB/Simulink for performance evaluation.
- [23] O. M. Arafa et al., "Performance analysis of a grid-connected inverter using Matlab/Simulink and real-time DSP implementation," IEEE Access, 2017. The study validates system behavior under various conditions.
- [24] M. Oettmeier et al., "Novel control strategy for four-quadrant inverters in low-power applications," IEEE Trans. Ind. Electron., 2010. Simulation and experimental results confirm efficiency improvements.
- [25] A. Chatterjee et al., "Comparative study of control techniques for grid-tied single-phase solar inverters," IEEE Trans. Ind. Electron., 2018. The research contrasts conventional and modern control methods.
- [26] H. Heydari-Doostabad et al., "High-speed deadbeat control for bidirectional buck-boost converters," IEEE Trans. Power Electron., 2018. The control strategy is validated through a 2.2-kW experimental prototype.
- [27] W. J. Huang et al., "Deadbeat current control for single-phase grid-connected inverters," IEEE Trans. Power Electron., 2007. Experimental results demonstrate fast response and grid synchronization.
- [28] Y. He et al., "Voltage sensor reduction and modulation improvement for grid-connected inverters," IEEE Trans. Power Electron., 2016. The study optimizes duty cycle values to mitigate current distortions.